Anisotropy of dielectric permittivity of $Sn_2P_2S_6$ measured with light-induced grating techniques

A. Shumelyuk, D. Barilov, S. Odoulov
Institute of Physics, National Academy of sciences, 46 Science Ave. 03 650 Kiev, Ukraine
shumeluk@iop.kiev.ua

E. Krätzig
Fachbereich Physik, Universität Osnabrück, Barbarastr. 7, 49076 Osnabrück, Germany
eckhard.kraetzig@uos.de

Abstract: Photorefractive grating spectroscopy is applied to study the anisotropy of the dielectric permittivity of $Sn_2P_2S_6$. Two techniques are used, one based on measurements of the amplitude of the space charge field grating as a function of grating spacing and the other based on measurements of the grating decay time. Both techniques provide close values for the anisotropy that appears to be well pronounced. The ratio of the dielectric permittivity in the [100] and the [001] direction is estimated to be close to 4. We found that the charge mobility is nearly the same along these two directions.
OCIS Codes: 190.5330, 190.7070

Introduction

Dynamic grating spectroscopy [1] opens a vast field for the investigation of defect and impurity centers and also of the charge transport dynamics in nonlinear crystals. It was used successfully for the determination of electrooptic and photovoltaic constants of photorefractive crystals, for the identification of the movable charge species, for the evaluation of the effective trap density and the identification of the spectra for donor and trap centers. We report in this paper on the application of grating spectroscopy for the analysis of the anisotropy of the dielectric constant in the relatively new wide bandgap photoreftractive crystal tin hypothiodiphosphate ($Sn_2P_2S_6$, SPS) [2]. The data on the dielectric permittivity are extracted from measurements of the dynamics of the space charge field gratings.

The space charge field, which is developing when a grating is recorded, is limited by the finite trap density and the dielectric constant of the crystal. By comparing the amplitudes of the space charge field for gratings aligned along two crystallographic axes we can get the ratio of the dielectric constants assuming the traps are distributed inside the crystal homogeneously. On the other hand, the decay of the space charge gratings occurs via usual Maxwell dielectric relaxation, i.e., because of finite conductivity σ. The characteristic decay time τ depends therefore on the dielectric permittivity ε, $\tau \propto \varepsilon\varepsilon_0/\sigma$. This provides an independent tool for the evaluation of ε.

Experiment

The SPS crystals have been grown via a gas transport reaction [2] in the Institute of Physics and Chemistry of the Solid State, University of Uzhgorod, Ukraine. The sample K3 cut along the crystallographic axes measures 9 x 9 x 4.5 mm^3, it has optically finished faces normal to the X - and Z -

directions. It belongs to the type I crystals [3,4] with a pronounced contribution of secondary carriers to the grating formation.

Two light beams from a TEM_{00} 40 mW He-Ne laser impinge upon the sample, either from the same face (transmission geometry) or from two opposite faces (reflection geometry). The orientation of the grating vector $\boldsymbol{K}$ remains the same for one set of measurements in transmission and reflection geometry; for the second set of measurements $\boldsymbol{K}$ is aligned along the other crystallographic axis and also remains the same for transmission and reflection geometry. The polarization of the light waves is normal to the plane of drawing in Fig. 1, the electric field vector of the light waves is always parallel to the $\boldsymbol{Y}$ axis.

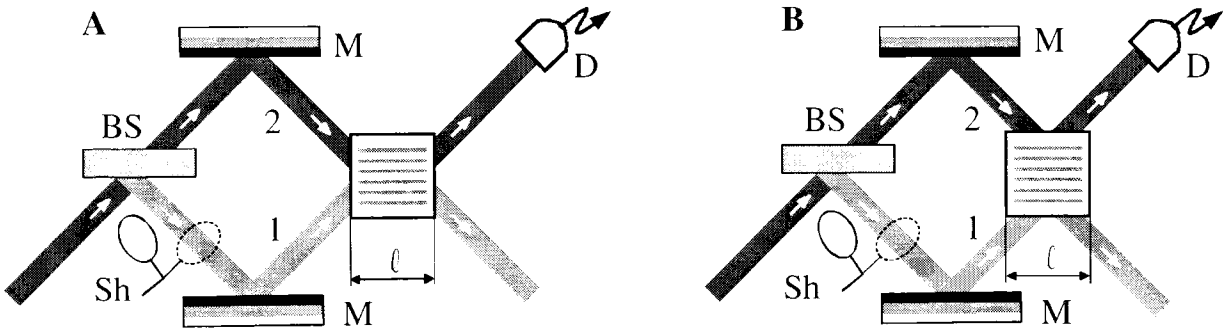

Fig. 1. Schematic representation of the experimental geometry to study the dynamics of recording in transmission (A) and reflection (B) geometry. D is a detector, Sh is a shutter, M are mirrors, BS is a beam splitter.

A typical temporal evolution of the intensity of one of the two recording beams (signal) during recording is as follows: At first the intensity of the transmitted signal beam is increasing till saturation because of beam coupling. Further exposure of the sample to the fringe pattern would result in a decrease of the light intensity because of formation of an out-of-phase grating by free carriers of opposite sign [5]. After the maximum intensity of the transmitted weak wave 1 is reached the input wave is stopped with a shutter placed in front of the sample. The initial intensity of the signal wave $I_1(0)$ and its saturated value $I_1(\ell)$ allow to evaluate the gain factor

$$\Gamma = \frac{1}{\ell} \ln\left[\frac{I_1(\ell)}{I_1(0)}\right]. \qquad (1)$$

Then the detector is measuring the decay of the intensity of the beam diffracted from the grating. By fitting this curve by an exponential function we obtain the decay time of the grating efficiency, which is half as large as the space charge decay time τ that we are searching for.

Further on, measurements of the gain factor and characteristic decay rates are performed for different angles of incidence of the recording waves to get the dependences $\Gamma = \Gamma(\Lambda)$ and $\tau^{-1} = \tau^{-1}(\Lambda)$, Λ being the fringe spacing. This is done for two orientations of the grating vector $\boldsymbol{K}$ parallel to the crystallographic axes, $\boldsymbol{K} \parallel \boldsymbol{X}$ and $\boldsymbol{K} \parallel \boldsymbol{Z}$.

Figure 2 represents the results of gain factor measurements. Empty dots and squares give the values measured in transmission grating geometry (see Fig. 1A), while filled dots and squares correspond

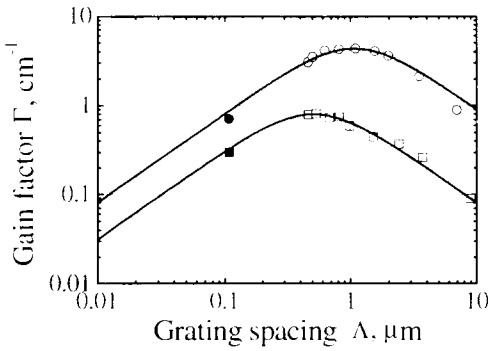

Fig. 2. Grating spacing dependences of the gain factor for a grating vector aligned along the sample's Z -axis (squares) and along the X -axis (dots). The recording light is polarized parallel to the Y –axis. Open dots and squares represent measurements with copropagating laser beams while filled dots and square corresponds to a counterpropagating beam geometry. Solid lines are best fits of the calculated dependence (Eq. 2).

to recording with counterpropagating waves (reflection grating geometry, see Fig. 1B). The dots represent values measured with $\boldsymbol{K} \parallel \boldsymbol{X}$ while data for $\boldsymbol{K} \parallel \boldsymbol{Z}$ are shown by squares.

The data on the grating decay rate presented in Fig. 3 are normalized to the light intensity, in fact

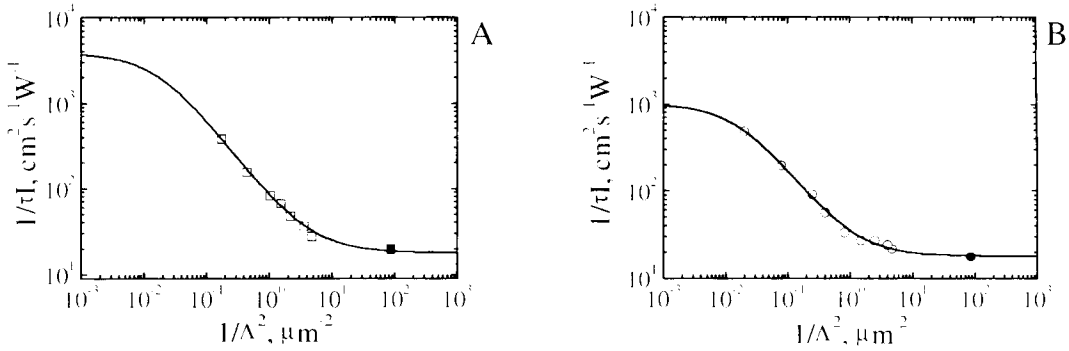

Fig. 3. Reciprocal decay time versus squared reciprocal grating spacing for a grating vector aligned along the samples Z-axis (A) and along X-axis (B). Open dots and squares represent measurements with copropagating laser beams while filled dots and squares corresponds to counterpropagating beam geometry. Solid lines are best fits of calculated

each value of $(1/\tau I)$ is extracted from the intensity dependence of the decay time $\tau = \tau(I)$ measured for a particular angle between the recording waves. The plot of $(1/\tau I)$ versus the squared reciprocal grating spacing simplifies the comparison to theoretical expression as will be discussed further. The meaning of open and filled dots and squares is the same as for Fig. 2.

Comparison with the theory

According to theory [6] the final expression for gain factor Γ reads

$$\Gamma = \frac{4\pi^2 n^3 r_{eff}}{\Lambda \lambda \cos\theta} \frac{k_B T}{e} \frac{1}{1 + \left(l_s/\Lambda\right)^2}, \qquad (2)$$

with the light wavelength λ in vacuum, the refraction index n, the effective electrooptic coefficient r_{eff}, the Boltzmann constant k_B, the absolute temperature T, the electron charge e, the angle 2θ between

the two recording waves (inside the crystal, the grating spacing $\Lambda = \lambda/2n\sin\theta$), and the Debye screening length

$$\ell_S = \sqrt{\frac{\varepsilon\varepsilon_0 k_B T}{e N_{eff}}}\ , \tag{3}$$

N_{eff} being the effective trap density. The gain factor reaches its maximum value at Λ equal to the Debye screening length ℓ_s. This allows for an experimental determination of ℓ_s which depends, as it follows from Eq. 3, on the dielectric permittivity ε.

The space charge grating can be erased by illumination of the sample. A light wave with the intensity I is exciting carriers and increases the conductivity σ. For any of the two types of carriers, the theory [7] predicts a single-exponential decay of the space charge grating with its own characteristic time τ

$$\frac{1}{\tau I} = \frac{\kappa}{\varepsilon\varepsilon_0}\frac{1+(\ell_s/\Lambda)^2}{1+(\ell_D/\Lambda)^2}\ . \tag{4}$$

Here κ is the specific photoconductivity, $\sigma = \kappa I$, and the diffusion length ℓ_D is given by the expression

$$\ell_D = \sqrt{D\tau_{fc}}\ , \tag{5}$$

where τ_{fc} is the free carrier lifetime and D is the diffusivity, related to the charge mobility μ via

$$D = \mu\frac{k_B T}{e}\ . \tag{6}$$

It follows from Eq. 4 that the dielectric permittivity enters twice Eq. 4, in the numerator (via ℓ_s, see Eq. 3) as also directly in the denominator. By changing the angle θ between the recording waves it is possible to vary Λ in a wide range and to meet either the condition $(\ell_s/\Lambda)>>1$ or $(\ell_s/\Lambda)<<1$. This offers several possibilities to extract the data on ε from the angular dependences of the decay rate. All measurements described in what follows have been done for the fast photorefractive grating that is formed in $Sn_2P_2S_6$ by photoexited holes [8].

The experimental data presented in Fig. 2 and Fig. 3 allow to extract the characteristic transport lengths, ℓ_s and ℓ_D. The first of these two lengths is determined from the position of the maximum of the $\Gamma = \Gamma(\Lambda)$ dependences (Fig. 2). We get $\ell_{sx} \approx 1.0$ μm for the X-direction while only $\ell_{sz} \approx 0.52$ μm for the Z-direction (extra subscripts for ℓ_s, z and x, respectively.) The data on the gain factor (Fig. 2) are also useful for the evaluation of the electrooptic tensor components.

The next step is to process the data of Fig. 3 by imposing the already known values of ℓ_{sx} and ℓ_{sz}. By fitting these data by Eq. 4 we extract the diffusion length for different crystallographic directions, $\ell_{Dx} \approx 7.5 \pm 0.2$ μm and $\ell_{Dz} \approx 7.8 \pm 1.0$ μm. Taking into account the definition of the diffusion length (Eq. 5, 6) we conclude that the anisotropy of charge mobility for charges involved in the formation of the fast grating in $Sn_2P_2S_6$ is rather small in the XOZ plane.

In addition, it is possible to evaluate the first factor in the right hand side of Eq. 4. The fit yields $(\kappa_{zz}/\varepsilon_{zz}\varepsilon_0) \approx 4\ 200$ cm^2/Ws and $(\kappa_{xx}/\varepsilon_{xx}\varepsilon_0) \approx 1\ 000$ cm^2/Ws. With a small difference in the charge mobilities the photoconductivity is nearly isotropic in the XOZ plane, too, $\kappa_{xx} \approx \kappa_{zz}$ and the anisotropy of $(\kappa/\varepsilon\varepsilon_0)$ can be attributed mainly to the anisotropy of the dielectric permittivity.

To get an estimate for the absolute value of ε one should know either the effective trap density N_{eff} or the specific photoconductivity κ. Both quantities need to be evaluated independently directly from electrical measurements what is out of the scope of the present paper. From the optical measurements that we performed we can get, however, the data on the anisotropy of the dielectric permittivity, i.e., the ratio $\varepsilon_{xx}/\varepsilon_{zz}$. This quantity can be extracted from the ratio of the Debye screening lengths

$$\frac{\varepsilon_{xx}}{\varepsilon_{zz}} = \left(\frac{\ell_{sx}}{\ell_{sz}}\right)^2 \approx 3.7 \pm 0.7\,, \tag{7}$$

and also from the ratio of the first factors in the right hand side of Eq. 4.

$$\frac{\varepsilon_{xx}}{\varepsilon_{zz}} \approx 3.9 \pm 0.2\,. \tag{8}$$

A reasonable agreement of the two estimates within the given range of the experimental accuracy is obvious.

Let us remind once more that it is necessary to know the anisotropy of the specific photoconductivity κ to evaluate $\varepsilon_{xx}/\varepsilon_{zz}$ using the second technique. It is important to underline that for the polarization used (normal to XOZ plane) the absorptivity does not depend on the orientation of the light beam in the XOZ plane for crystals with the symmetry *m*. With a rather small (if any) anisotropy of the mobility, the photoconductivity κ is nearly isotropic, too.

An independent check of the validity of the second proposed technique is as follows: In the limit of small grating spacing, $\Lambda \to 0$, i.e., $(\ell_s/\Lambda) >> 1$, one can neglect the unity in the numerator as well as in the denominator of the second factor in the right hand side of Eq. 4 and arrive at

$$\frac{1}{\tau I} = \frac{\ell_s^2}{\varepsilon\varepsilon_0}\frac{\kappa}{\ell_D^2}\,. \tag{9}$$

From the definition of the Debye screening length (Eq. 3) it is clear that the first factor in Eq. 9, $(\ell_s^2/\varepsilon\varepsilon_0)$, does not depend on the dielectric permittivity. It is easy to check also that the second factor (κ/ℓ_D^2) does not depend on a possible anisotropy of the free carrier mobility. From symmetry considerations it follows that the absorption constant for light polarised along the *Y* -axis is isotropic in XOZ plane. Thus the right hand side of Eq. 9 contains no anisotropic quantities and should therefore be the same for an arbitrary orientation of the grating vector.

For the small spacing limit our fits give the same values $(1/\tau I) \approx 18.0$ cm^2/Ws measured along the *Z* -axis and along the *X* -axis. Taking into account that $(1/\tau I)$ varies more than two orders of magnitude within the whole range of grating spacing variation this coincidence can hardly be accidental and is in agreement with our expectations.

In crystals belonging to the symmetry class m the electrooptic coefficients r_{112}, r_{222} *and* r_{332} *are zero* and self-diffraction from space charge gratings with the grating vector aligned along the Y -axis is impossible. This is the reason why we report on the anisotropy of the $Sn_2P_2S_6$ parameters in the XOZ plane only. In principle, the nonvanishing electrooptic coefficients r_{232} and r_{212} allow for anisotropic diffraction with the polarization of the diffracted wave orthogonal to the polarization of the readout wave. To observe this type of diffraction one should ensure, however, appropriate Bragg angles that do not coincide with the recording angles.

Conclusions

By using all-optical techniques based on the study of the dynamics of grating recording and erasure we discovered a strong anisotropy of the dielectric permittivity in tin hypothiodiphosphate ($Sn_2P_2S_6$) at ambient temperature, $\varepsilon_{xx}/\varepsilon_{zz} \approx 4$. It follows from our measurements that the photoextited hole mobility is nearly insensitive of direction in the same plane, $\mu_{xx}/\mu_{zz} \approx 1$. We were informed recently that our data on the anisotropy, $\varepsilon_{xx}/\varepsilon_{zz} \approx 4$, are in good agreement with the results of direct measurements of the dielectric permittivity in SPS, published unfortunately in hardly accessible scientific journal [9].

The grating spectroscopy techniques allow also for the evaluation of the anisotropy of the electrooptic properties [5]. Our estimates give rather small values $\xi r_{221} \approx 17$ pm/V and $\xi r_{223} \approx 2$ pm/V ($\xi < 1$ being a factor that takes into account a possible imperfect poling of the same). It should be underlined that these relatively weak components were selected deliberately for the measurements of the ε -anisotropy: First, we were well within the undepleted pump approximation when measuring gain factors, second, just these components are involved in recording of both, transmission and reflection gratings and last but not least there is no absorption anisotropy for the chosen geometry and light polarization.

Acknowledgements Support of the Alexander von Humboldt Foundation is gratefully acknowledged. We are grateful to Dr. A. Grabar for the $Sn_2P_2S_6$ sample and for fruitful discussions.

References

1. H. J. Eichler, P. Gunter, and D. W. Pohl, *Laser-induced dynamic gratings* (Springer-Verlag, Berlin 1986).
2. C. D. Carpenter and A. Nitche, Materials Research Bulletin 9 401-410 (1974).
3. A. Shumelyuk, S. Odoulov, G. Brost, U. Hellwig, Yi Hu, and E. Krätzig, Ti-sapphire laser beamcoupling in $Sn_2P_2S_6$, CLEO'98 Technical Digest, pp. 171-172, (San-Francisco, May 1998).
4. A. Shumelyuk, S. Odoulov, D. Kip, and E. Krätzig, Appl. Phys. B 72 707-710 (2001).
5. S. Odoulov, A. Shumelyuk, U. Hellwig, R. Rupp, A. Grabar, and I. Stoyka, J. Opt. Soc. Am. B 13 2352 – 2360 (1996).
6. N. Kukhtarev, V. Markov, S. Odoulov, M. Soskin, and V. Vinetskii, Ferroelectrics 22 949-960 (1979).
7. F. P. Strohkendl, J. M. C. Jonathan, R. W. Hellwarth, Opt. Lett. 11 312-314 (1986).
8. I. Seres, S. Stepanov, S. Mansurova, and A. Grabar, J. Opt. Soc. Am. B 17 1986-1991 (2000).
9. V. M. Kedyulich, A. G. Slivka, E. I. Gerzanich, P. P. Guranich,V. S. Shusta, and P. M. Lucach, Uzhgorod University Bulletin, Phys. Ser. 5 30-32 (1995).